Dirac quasinormal frequencies in Schwarzschild-AdS space-time

M. Giammatteo[*]

School of Mathematics and Statistics, University of Newcastle upon Tyne, Newcastle upon Tyne NE1 7RU, United Kingdom

Jiliang Jing[†]

Institute of Physics and Department of Physics, Hunan Normal University, Changsha, Hunan 410081 P. R. China

We investigate the quasinormal mode frequencies for the massless Dirac field in static four dimensional *AdS* space-time. The separation of the Dirac equation is achieved for the first time in *AdS* space. Besides the relevance that this calculation can have in the framework of the *AdS/CFT* correspondence between M-theory on $AdS_4 \times S^7$ and SU(N) super Yang-Mills theory on M_3, it also serves to fill in a gap in the literature, which has only been concerned with particles of integral spin 0, 1, 2.

I. INTRODUCTION

Perturbations of black holes are dominated, over intermediate time-scales, by characteristic modes known as quasinormal modes. They are similar to normal modes of a closed system, but since the field can fall into the black hole or radiate to infinity, the modes decay and the corresponding frequencies are complex [1]. They have been extensively studied in asymptotically flat space-times and good reviews on the topic can be found in [2,3]. The study of quasinormal modes in Anti-de Sitter space was first done in [4].

More recently quasinormal frequencies have been investigated in the context of string theory in Anti-de Sitter space [5–7]. There is a suggestion, known as *AdS/CFT* correspondence, that string theory in Anti-de Sitter space is equivalent to a conformal field theory in one dimension fewer [8]. In the framework of this conjecture the study of *AdS* black holes has a direct interpretation in terms of the dual conformal field theory on its boundary. The duality predicts that the retarded *CFT* correlation functions are in one to one correspondence with Green's functions on Anti-de Sitter space with appropriate boundary conditions [9–12]. Furthermore, as mentioned in [5], it is assumed that a large static black hole in *AdS* space corresponds to a thermal state in the *CFT* on the boundary. Perturbing the black hole is equivalent to perturbing this thermal state. The perturbed system is expected, at late times, to approach equilibrium exponentially with a characteristic time-scale. This time-scale is inversely proportional to the imaginary part of the poles of the correlators of the perturbation operator. It seems that these relaxation time-scales are quite complicated to calculate in the *CFT*, therefore their computation is conveniently replaced by the evaluation of the quasinormal frequencies in the *AdS* bulk space. In [6,7], the authors went beyond the scalar perturbation treated in [5] and they considered electromagnetic and gravitational perturbations. In one of the most

recent works on the subject, Berti and Kokkotas [13] confirm and extend previous results on scalar, electromagnetic and gravitational perturbations of static *AdS* black holes and analyze, for the first time, Reissner-Nordstrom Anti-de Sitter black holes and calculate their quasinormal frequencies.

The interaction of a Dirac field with a black hole has been studied by Finster and his collaborators in a series of papers. While they have found stable particlelike solutions in the Einstein-Dirac- Maxwell system [14,15], they have also proved the nonexistence of time-periodic solutions in various black hole space-times [16,17]. This means that Dirac particles, including electrons and neutrinos, cannot remain on a periodic orbit around a black hole. In [18], they also showed that there are no spherical symmetric black hole solutions in the Einstein-Dirac-Maxwell system other than the Reissner-Nordström one. This suggests that if a cloud of Dirac particles undergoes gravitational collapse, the fermionic particles either vanish inside the event horizon of a black hole or escape to infinity.

The quasinormal frequencies related to the evolution of a massless Dirac field in a Schwarzschild black hole space-time, were studied in [19]. The quasinormal modes of the Reissner-Nordström de Sitter black hole for Dirac fields were studied by using the Pöshl-Teller potential approximation in Ref. [20]. In this paper we are interested in the analysis of the modes of vibration of a massless Dirac field in a Schwarzschild Anti-de Sitter background space and it is for this reason that we compute the related quasinormal mode frequencies. This calculation is relevant to the *AdS/CFT* correspondence between M-theory on $AdS_4 \times S^7$ and $SU(N)$ super Yang-Mills theory on M_3, and it also serves to fill in a gap in the literature, which, in *AdS* spaces, has only been concerned with particles of integral spin 0, 1, 2.

II. DIRAC EQUATION IN STATIC ADS SPACE-TIME

The metric for a Schwarzschild Anti-de Sitter black hole can be written as

---

*Electronic address: mgiammatteo@hotmail.com
†Electronic address: jljing@hunnu.edu.cn

$$ds^2 = -f dt^2 + \frac{1}{f} dr^2 + r^2(d\theta^2 + \sin^2\theta d\varphi^2), \quad (2.1)$$

with

$$f = 1 - \frac{2M}{r} - \frac{\Lambda}{3} r^2, \quad (2.2)$$

where the parameters M, and Λ represent the black hole mass, and the negative cosmological constant, respectively.

The Dirac equation in a general background space-time can be written, according to [21], as

$$[\gamma^a e_a^\mu (\partial_\mu + \Gamma_\mu)]\Psi = 0. \quad (2.3)$$

Here, γ^a are the Dirac matrices,

$$\gamma^0 = \begin{pmatrix} -i & 0 \\ 0 & i \end{pmatrix}, \quad \gamma^i = \begin{pmatrix} 0 & -i\sigma^i \\ i\sigma^i & 0 \end{pmatrix}, \quad i = 1, 2, 3, \quad (2.4)$$

while σ^i are the Pauli matrices,

$$\sigma^1 = \begin{pmatrix} 0 & 1 \\ 1 & 0 \end{pmatrix}, \quad \sigma^2 = \begin{pmatrix} 0 & -i \\ i & 0 \end{pmatrix}, \quad \sigma^3 = \begin{pmatrix} 1 & 0 \\ 0 & -1 \end{pmatrix}. \quad (2.5)$$

The four-vectors e_a^μ represent the inverse of the tetrad e_a^μ defined by the metric $g_{\mu\nu}$ as,

$$g_{\mu\nu} = \eta_{ab} e_\mu^a e_\nu^b, \quad (2.6)$$

with $\eta_{ab} = \text{diag}(-1, 1, 1, 1)$ being the Minkowski metric. Γ_μ are the spin connection coefficients, which are given by

$$\Gamma_\mu = \frac{1}{8}[\gamma^a, \gamma^b] e_a^\nu e_{b\nu;\mu}. \quad (2.7)$$

Here, $e_{b\nu;\mu} = \partial_\mu e_{b\nu} - \Gamma_{\mu\nu}^\alpha e_{b\alpha}$ is the covariant derivative of $e_{b\nu}$ and $\Gamma_{\mu\nu}^\alpha$ is the Christoffel symbol.

We take the tetrad to be

$$e_\mu^a = \text{diag}\left(\sqrt{f}, \frac{1}{\sqrt{f}}, r, r\sin\theta\right). \quad (2.8)$$

The spin connection Γ_μ can then be expressed as

$$\Gamma_0 = \frac{1}{4} f' \gamma_0 \gamma_1, \Gamma_1 = 0, \Gamma_2 = \frac{1}{2}\sqrt{f}\gamma_1\gamma_2, \Gamma_3$$

$$= \frac{1}{2}(\sin\theta\sqrt{f}\gamma_1\gamma_3 + \cos\theta\gamma_2\gamma_3). \quad (2.9)$$

The Dirac Eqs. (2.3) become

$$-\frac{\gamma_0}{\sqrt{f}} \frac{\partial\Psi}{\partial t} + \sqrt{f}\gamma_1\left(\frac{\partial}{\partial r} + \frac{1}{r} + \frac{1}{4f}\frac{df}{dr}\right)\Psi$$

$$+ \frac{\gamma_2}{r}\left(\frac{\partial}{\partial\theta} + \frac{1}{2}\cot\theta\right)\Psi + \frac{\gamma_3}{r\sin\theta}\frac{\partial\Psi}{\partial\varphi} = 0. \quad (2.10)$$

If we rescale Ψ as

$$\Psi = f^{-\frac{1}{4}}\Phi, \quad (2.11)$$

Eq. (2.10) assumes a simpler form in the new unknown Φ, which can be written as

$$-\frac{\gamma_0}{\sqrt{f}} \frac{\partial\Phi}{\partial t} + \sqrt{f}\gamma_1\left(\frac{\partial}{\partial r} + \frac{1}{r}\right)\Phi + \frac{\gamma_2}{r}\left(\frac{\partial}{\partial\theta} + \frac{1}{2}\cot\theta\right)\Phi$$

$$+ \frac{\gamma_3}{r\sin\theta}\frac{\partial\Phi}{\partial\varphi} = 0. \quad (2.12)$$

We introduce a well known coordinate change from the radial variable r to the tortoise coordinate r_* given by

$$r_* = \int \frac{dr}{f}. \quad (2.13)$$

We will use an ansatz for the Dirac spinor

$$\Phi = \begin{pmatrix} \frac{iG^{(\pm)}(r)}{r} \phi_{jm}^{\pm}(\theta, \varphi) \\ \frac{F^{(\pm)}(r)}{r} \phi_{jm}^{\mp}(\theta, \varphi) \end{pmatrix} e^{-i\omega t}, \quad (2.14)$$

with spinor angular harmonics

$$\phi_{jm}^+ = \begin{pmatrix} \sqrt{\frac{j+m}{2j}} Y_l^{m-1/2} \\ \sqrt{\frac{j-m}{2j}} Y_l^{m+1/2} \end{pmatrix}, \quad \left(\text{for } j = l + \frac{1}{2}\right), \quad (2.15)$$

$$\phi_{jm}^- = \begin{pmatrix} \sqrt{\frac{j+1-m}{2j+2}} Y_l^{m-1/2} \\ -\sqrt{\frac{j+1+m}{2j+2}} Y_l^{m+1/2} \end{pmatrix}, \quad \left(\text{for } j = l - \frac{1}{2}\right). \quad (2.16)$$

Note that $Y_l^{m\pm1/2}(\theta, \varphi)$ represent ordinary spherical harmonics. Since

$$\begin{pmatrix} -i(\frac{\partial}{\partial\theta} + \frac{1}{2}\cot\theta) & \frac{1}{\sin\theta}\frac{\partial}{\partial\varphi} \\ -\frac{1}{\sin\theta}\frac{\partial}{\partial\varphi} & i(\frac{\partial}{\partial\theta} + \frac{1}{2}\cot\theta) \end{pmatrix} \begin{pmatrix} \phi_{jm}^{\pm} \\ \phi_{jm}^{\mp} \end{pmatrix}$$

$$= i\begin{pmatrix} k_\pm & 0 \\ 0 & k_\pm \end{pmatrix} \begin{pmatrix} \phi_{jm}^{\pm} \\ \phi_{jm}^{\mp} \end{pmatrix}, \quad (2.17)$$

Eqs. (2.12) can be written in the simplified matrix form

$$\begin{pmatrix} 0 & -\omega \\ \omega & 0 \end{pmatrix}\begin{pmatrix} F^\pm \\ G^\pm \end{pmatrix} - \frac{\partial}{\partial r_*}\begin{pmatrix} F^\pm \\ G^\pm \end{pmatrix} + \sqrt{f}\begin{pmatrix} \frac{k_\pm}{r} & 0 \\ 0 & -\frac{k_\pm}{r} \end{pmatrix}\begin{pmatrix} F^\pm \\ G^\pm \end{pmatrix}$$

$$= 0. \quad (2.18)$$

These equations can be thought of as equations referring to the radial functions (F^+, G^+) or (F^-, G^-) depending on the original choice made in the ansatz of Eq. (2.14). On the other hand it can be proved that the radial differential equations related to the two different sets of functions are exactly the same. In other words, we have a unique equation for $F^\pm$ and another equation for $G^\pm$. For this reason we will avoid from now on specifying if we are referring to the spin up or spin down components when talking about $F^\pm$ and $G^\pm$ and we will simply call these functions F and G. Consequently the two decoupled equations can be expressed in the form

$$\frac{d^2 F}{dr_*^2} + (\omega^2 - V_1)F = 0, \qquad (2.19)$$

$$\frac{d^2 G}{dr_*^2} + (\omega^2 - V_2)G = 0, \qquad (2.20)$$

with

$$V_1 = \frac{\sqrt{f}|k|}{r^2}\left(|k|\sqrt{f} + \frac{r}{2}\frac{df}{dr} - f\right),$$

$$\left(k = j + \frac{1}{2}, j = l + \frac{1}{2}\right) \qquad (2.21)$$

$$V_2 = \frac{\sqrt{f}|k|}{r^2}\left(|k|\sqrt{f} - \frac{r}{2}\frac{df}{dr} + f\right),$$

$$\left(k = -j - \frac{1}{2}, j = l - \frac{1}{2}\right). \qquad (2.22)$$

In a similar way to the integer spin case in [19], the two potentials V_1 and V_2, are supersymmetric partners derived from the same superpotential. In the asymptotically flat case, it has been shown that potentials related in this way possess the same spectra of quasinormal mode frequencies [22]. In the AdS case, this is still true provided that the boundary conditions are mapped between the two cases in a consistent way. We shall concentrate just on Eq. (2.19) with potential V_1 in evaluating the quasinormal mode frequencies in the next section.

III. DIRAC QUASINORMAL FREQUENCIES

In this section we evaluate the quasinormal frequencies for the massless Dirac field using the Frobenius series solution method. We start defining Δ as

$$\Delta = r^2 - 2Mr + \alpha^2 r^4, \qquad (3.1)$$

where $\alpha^2 = -\Lambda/3$. This implies that the function f in (2.19) can be rewritten as $f = \Delta/r^2$. Next, rescale F as

$$F = e^{-i\omega r_*}u, \qquad (3.2)$$

which allows us to scale out the behavior of the function at the black hole event horizon. We obtain an equation in u given by

$$f^2\frac{d^2 u}{dr^2} + \left\{f\frac{df}{dr} - 2i\omega f\right\}\frac{du}{dr} - Vu = 0. \qquad (3.3)$$

Let us now set

$$r = \frac{1}{x}. \qquad (3.4)$$

We obtain the equation in the variable x

$$f^2 x^4 \frac{d^2 u}{dx^2} + f x^2\left(2xf + x^2\frac{df}{dx} + 2i\omega\right)\frac{du}{dx} - Vu = 0. \qquad (3.5)$$

Define p as

$$p = x^2 - 2Mx^3 + \alpha^2 x^4. \qquad (3.6)$$

Note that $p_1 = p(x_1) = \Delta(x_1)x_1^4 = 0$. Rescale f as

$$f = \Delta x^2 = px^{-2} \qquad (3.7)$$

inserting this into (3.5) we obtain the equation

$$p^2\frac{d^2 u}{dx^2} + p\left(\frac{dp}{dx} + 2i\omega\right)\frac{du}{dx} - Vu = 0. \qquad (3.8)$$

Rescale again the independent variable x, by introducing the variable z given by

$$\left(\frac{x_1 - x}{x_1}\right) = z^2, \qquad (3.9)$$

we obtain a new expression for V in the variable z,

$$V(z) = p|k|^2 + p^{1/2}|k|x_1(1 - z^2)[3Mx_1(1 - z^2) - 1]. \qquad (3.10)$$

Insert (3.9) into (3.8) and rescale all the parameters: M, α^2, ω with respect to x_1, which is the inverse of the radial coordinate r_1 of the black hole event horizon, while r_1 is the largest root of Δ. We obtain

$$\hat{p}z\frac{d^2 u}{dz^2} - \left\{\hat{p} - \frac{d\hat{p}}{dz}z + 4i\hat{\omega}z^2\right\}\frac{du}{dz} - 4z^3\{|k|^2$$
$$+ \hat{p}^{-1/2}[3\hat{M}|k|(1 - z^2)^2 - |k|(1 - z^2)]\}u = 0, \qquad (3.11)$$

where

$$\hat{p} = px_1^{-2}. \qquad (3.12)$$

Expanding the coefficients of Eq. (3.11) as Taylor series around $z = 0$, which is the same than performing a series expansion around the black hole event horizon, we obtain

$$A(z)\frac{d^2 u}{dz^2} - B(z)\frac{du}{dz} - C(z)u = 0, \qquad (3.13)$$

where

$$A(z) = p_2 z^3 + p_3 z^5 + 2\hat{M}z^7, \qquad (3.14)$$

$$B(z) = (4i\hat{\omega} - p_2)z^2 - 3p_3 z^4 - 10\hat{M}z^6, \qquad (3.15)$$

$$C(z) = 4|k|^2 z^3 + 2|k|p_2 z^2\hat{q}^{-1/2} + 4|k|p_3 z^4\hat{q}^{-1/2}$$
$$+ 12\hat{M}|k|z^6\hat{q}^{-1/2}, \qquad (3.16)$$

with

$$p_2 = (6\hat{M} - 2), \qquad (3.17)$$

$$p_3 = (-6\hat{M} + 1) \qquad (3.18)$$

and

$$\hat{q} = \hat{p}z^{-2} = p_2 + p_3 z^2 + 2\hat{M}z^4. \qquad (3.19)$$

The differential equation in u can be now solved by series by exploiting Frobenius method, which consists in looking for a solution of the form

$$u = z^\rho \sum_{n=0}^{\infty} a_n z^n. \quad (3.20)$$

The main difference between the spin $\frac{1}{2}$ case and the integer spin case is the nonpolynomial term $\hat{q}^{-1/2}$. This function can be Taylor expanded as

$$\hat{q}^{-1/2} = (p_2 + p_3 z^2 + 2\hat{M}z^4)^{-1/2} = \sum_{s=0}^{\infty} \frac{1}{s!} A_s z^s, \quad (3.21)$$

leaving aside for the moment the problem of deriving the coefficients of this last series.

The two possible values for the index ρ at $z = 0$ of our series solution (3.20) can be easily calculated and they are given by $\rho_1 = 0$ and $\rho_2 = 4i\hat{\omega}/p_2$. We pick the first of the indices (the other solution has infinitely many oscillations close to the horizon) and therefore look for a series solution which will be simply given by

$$u = \sum_{n=0}^{\infty} a_n z^n. \quad (3.22)$$

The infinite nature of the expansion for $\hat{q}^{-1/2}$ and u, leads us to deal with a product of two series which can be expressed as a single series,

$$\left(\sum_{s=0}^{\infty} \frac{1}{s!} A_s z^s\right)\left(\sum_{n=0}^{\infty} a_n z^n\right) = \sum_{n=0}^{\infty}\left(\sum_{s=0}^{n} \frac{1}{s!} A_s a_{n-s}\right) z^n. \quad (3.23)$$

Inserting Eqs. (3.22) and (3.23) into Eq. (3.13), we obtain a recurrence relation for a_{n+1} which has n terms,

$$-4|k|p_3\left\{A_0 a_{n-2} + \cdots + \frac{A_{n-2}}{(n-2)!}a_0\right\}$$

$$-12\hat{M}|k|\left\{A_0 a_{n-4} + \cdots + \frac{A_{n-4}}{(n-4)!}a_0\right\} = 0.$$

This recurrence equation, due to its unbounded character caused by the series expansion for $\hat{q}^{-1/2}$, is much harder to solve by numerical recursion, and in any case before we proceed we first need to know the expression for the coefficients A_s of the Taylor expansion of $\hat{q}^{-1/2}$. This problem is solved by remembering Faà di Bruno's formula for the analytical calculation of derivatives of any order

$$h_n = \left[\frac{d^n h}{dx^n}\right]_{x=x_0} = \sum_{k=1}^{n} f_k \sum_{p(n,k)} n! \prod_{i=1}^{n} \frac{g_i^{a_i}}{(a_i!)(i!)^{a_i}}, \quad (3.25)$$

where $h(x) = f[g(x)]$ is a composed function,

$$f_k = \frac{d^k}{dy^k}f(y_0) \quad (3.26)$$

and

$$g_i = \frac{d^i}{dx^i}g(x_0). \quad (3.27)$$

The second sum inside (3.25) is done over partitions $p(n, k)$, which are defined as

$$p(n, k) = \left\{(a_1, \ldots, a_n) : a_i \in \mathcal{N}_0, \sum_{i=1}^{n} a_i = k, \sum_{i=1}^{n} ia_i = n\right\}, \quad (3.28)$$

where $\mathcal{N}_0$ is equal to the set of non-negative integers. An element $(a_1, \ldots, a_n)$ belonging to $p(n, k)$ represents a partition of a set with n elements into a_1 classes of cardinality $1, \ldots, a_n$ classes of cardinality n. The number of such partitions is represented by the Stirling numbers of the second kind,

$$S_n^{(k)} = \sum_{p(n,k)} n! \prod_{i=1}^{n} \frac{1}{(a_i!)(i!)^{a_i}}. \quad (3.29)$$

When formula (3.25) is applied to the A_s coefficients, we have

$$A_s = \sum_{m=1}^{s} f^{(m)}[\hat{q}(0)] \sum_{p(s,m)} s! \prod_{i=1}^{s} \frac{1}{(a_i!)(i!)^{a_i}}\{\hat{q}^{(i)}(0)\}^{a_i}, \quad (3.30)$$

with $f^{(m)}[\hat{q}(0)]$ given by

$$\prod_{k=0}^{m-1}\left(-\frac{(2k+1)}{2}\right)[\hat{q}(0)]^{-1/2-m}. \quad (3.31)$$

On the other hand, evaluating $\hat{q}$ and its derivatives at $z = 0$, we obtain

$$\hat{q}(0) = 6\hat{M} - 2, \quad (3.32)$$

$$\hat{q}''(0) = 2(1 - 6\hat{M}), \quad (3.33)$$

$$\hat{q}^{(4)}(0) = 48\hat{M}, \quad (3.34)$$

while

$$\hat{q}'(0) = \hat{q}'''(0) = 0, \quad (3.35)$$

beside all the derivatives of order higher than four. The A_s coefficients can then be written in the form

$$A_s = \sum_{m=1}^{s} f^{(m)}[\hat{q}(0)]s!\left\{\left[\frac{1}{(a_2!)(2!)^{a_2}}\{\hat{q}''(0)\}^{a_2}\right]\right.$$

$$\left.\times \left[\frac{1}{(a_4!)(4!)^{a_4}}\{\hat{q}^{(4)}(0)\}^{a_4}\right]\right\}, \quad (3.36)$$

where the set of partitions $p(s, m)$ now contains only a single element

$$p(s, m) = \{(a_2, a_4) : a_2, a_4 \in \mathcal{N}_0, a_2 + a_4$$
$$= m, 2a_2 + 4a_4 = s\}. \tag{3.37}$$

Hence

$$a_2 = 2m - \frac{1}{2}s \tag{3.38}$$

$$a_4 = \frac{1}{2}s - m, \tag{3.39}$$

for $4m > s > 2m$ and s even. Expression (3.36) is very simple to encode in a numerical subroutine.

A. Boundary conditions

Having separated Dirac equations in Anti-de Sitter Schwarzschild black hole background spaces and obtained two radial second order differential Eqs. (2.19) and (2.20), we have argued that those two equations are related. They can be physically identified as the equations governing the axial and polar perturbations of the Dirac field, respectively. We have also mentioned the fact that the two potentials (2.21) and (2.22) possess the same quasinormal mode frequency spectra if the boundary conditions are mapped consistently.

According to Cooper [23], Eq. (2.19) describes axial perturbations and Eq. (2.20) describes polar perturbations of the Dirac field. Suppose we are interested in investigating further the AdS/CFT conjecture and want to relate the spinor field and its quasinormal frequencies to the calculation of the correlation functions on the boundary conformal field theory. More precisely, let us suppose that we are interested in evaluating the correlators of a polar quantity in the CFT on the boundary, which corresponds to the polar part of the spinor field in the bulk of AdS space-time. Accordingly we must set the *axial* spinor field perturbation to vanish on the boundary.

In terms of what we have done until now, we must take our series solution (3.22) to the axial Eq. (2.19), and impose on this Dirichlet boundary conditions

$$u(z) = \sum_{n=0}^{\infty} a_n z^n \to 0 \tag{3.40}$$

as $z \to 1$. Taking the limit of the left hand side gives us the identity

$$\sum_{n=0}^{\infty} a_n = 0. \tag{3.41}$$

This is an implicit equation for the computation of quasinormal frequencies related to the spinor field. The computer program which performs the numerical calculation is organized in the following way. An independent routine evaluates the coefficients A_s associated to the Taylor expansion of $\hat{q}^{-1/2}$. These results are then exploited within a recursive routine which iterates the recurrence relation to
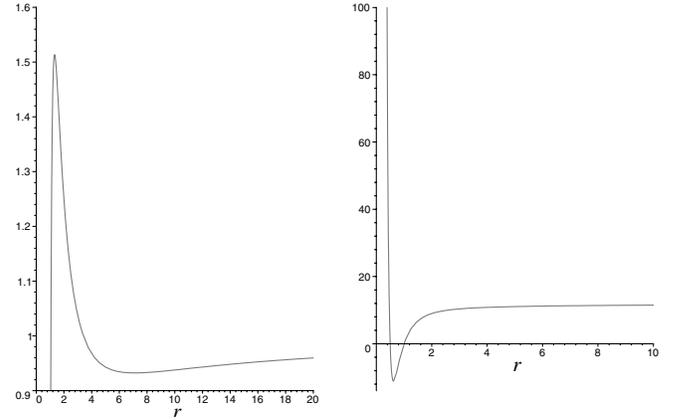

FIG. 1. In this figure we show the potentials related to axial perturbations of AdS Schwarzschild black holes. The plot on the left represents the potential related to the evolution of an axial spin-$\frac{1}{2}$ field, for $l = 0$ and $\hat{M} = 1.0$. The plot on the right represents the potential related to the evolution of an axial spin-2 field, for $l = 3$ and $\hat{M} = 1.0$. The masses are rescaled with respect to the radial coordinate of the black hole event horizons.

evaluate the coefficients a_n of the series solution. Finally, an ordinary Newton-Raphson root-finding routine seeks for solutions to the Eq. (3.41).

The choice of boundary conditions is related to the axial or polar character of the spinor field at infinity and to its interpretation in terms of the AdS/CFT conjecture. On the other hand the consistency of the boundary conditions can be checked by the shape of the effective potential in the differential Eq. (2.19) we are solving.

In Fig. 1, we plot the potential related to the evolution of the axial component of massless spin-$\frac{1}{2}$ fields alongside the axial potential for the spin-2 case in four dimensional Schwarzschild-AdS space-time. Note that $r \to \infty$ is a regular point of the differential Eq. (2.19) and Dirichlet boundary conditions are a consistent choice.

IV. NUMERICAL RESULTS

The numerical procedure described above can be successfully applied to both large black holes, for which the radius of the event horizon r_1 is much larger than the Anti-de Sitter radius α^{-1} ($r_1 >> \alpha^{-1}$), and intermediate black holes for which $r_1 \sim \alpha^{-1}$. The quasinormal frequencies are decomposed into real and imaginary parts

$$\omega = \omega_R + i\omega_I. \tag{4.1}$$

With this sign chosen, ω_I is negative for all quasinormal frequencies. In Table I, we list the values of the lowest quasinormal mode frequencies for $\alpha^{-1} = 1$, $l = 0$ and selected values of r_1. For large black holes, the real and imaginary parts of the frequency scale linearly with the horizon radius, resembling the results obtained in [5,6] for other perturbation fields. Since the temperature scales also

TABLE I. Values of the lowest Dirac quasinormal mode frequency for $\alpha^{-1} = 1.0$ and $n = 0, l = 0$. These results are obtained by evaluating the frequency as a function of r_1 for some selected black hole sizes.

r_1	ω_R	ω_I	r_1	ω_R	ω_I
100	~0	−76.8157	1.0	1.80808	−1.10565
60	~0	−46.8901	0.8	1.76332	−0.8516
40	~0	−31.9303	0.5	1.7463	−0.4525
20	~0	−17.0652	0.45	1.7555	−0.3829
10	~0	−10.0749	0.4	1.7719	−0.3118
5	2.20	−6.3626	0.3	1.7958	−0.1768

with r_1 in this regime, the imaginary part of the frequency, which determines how damped the mode is and which according to the AdS/CFT correspondence is a measure of the characteristic time $\tau = 1/|\omega_I|$ of approach to thermal equilibrium, scales with the temperature. Therefore, in the dual CFT the approach to thermal equilibrium is faster for higher temperatures. The linearity of the scaling between ω_I and T is clearly shown in Fig. 2, both for the $n = 0$ and $n = 1$ mode numbers. The dots represent some frequencies numerically calculated. The lines connecting them are linear fits. Explicitly, the lines are given by

$$\omega_I = -3.11T \tag{4.2}$$

for $n = 0$ and

$$\omega_I = -9.36T \tag{4.3}$$

for $n = 1$.

In Table II, we list the values of the first 11 quasinormal mode frequencies corresponding to massless spinor perturbations of large Schwarzschild-AdS black holes ($r_1 \gg \alpha^{-1}$). For large values of the overtone number n, the frequencies become evenly spaced in mode number and

TABLE II. Quasinormal mode frequencies corresponding to $l = 0$ and $l = 1$ massless Dirac perturbations of a large Schwarzschild-AdS black hole ($r_1 = 100$). For large values of the overtone number n, the modes become evenly spaced in mode number and the spacing is given by $\frac{(\omega_{n+1} - \omega_n)}{r_1} \sim (1.299 - 2.25i)$.

Overtone Number	$l = 0$		$l = 1$	
n	ω_R	ω_I	ω_R	ω_I
0	~ 0	−76.8402	~ 0	−78.7731
1	~ 0	−217.83	~ 0	−211.417
2	47.7354	−417.775	76.7222	−406.192
3	178.073	−650.494	203.247	−636.479
4	305.383	−877.767	330.457	−863.679
5	433.279	−1104.39	458.292	−1090.25
6	561.539	−1330.64	586.517	−1316.47
7	690.04	−1556.66	715.01	−1542.46
8	818.77	−1782.56	843.695	−1768.29
9	947.614	−2008.24	972.531	−1994.02
10	1076.56	−2233.86	1101.48	−2219.65

the spacing, which is independent of the angular mode number l, is given by

$$\frac{(\omega_{n+1} - \omega_n)}{r_1} \sim (1.299 - 2.25i). \tag{4.4}$$

This is exactly the same spacing, related to the large black hole regime, obtained by Cardoso and his collaborators in [24], for different kinds of perturbing fields. Their results were the same for scalar, electromagnetic and gravitational perturbations. Moreover, the quasinormal frequencies of large black holes have a number of first overtones with pure imaginary parts as in the electromagnetic and gravitational cases. The higher the black hole radius r_1, the
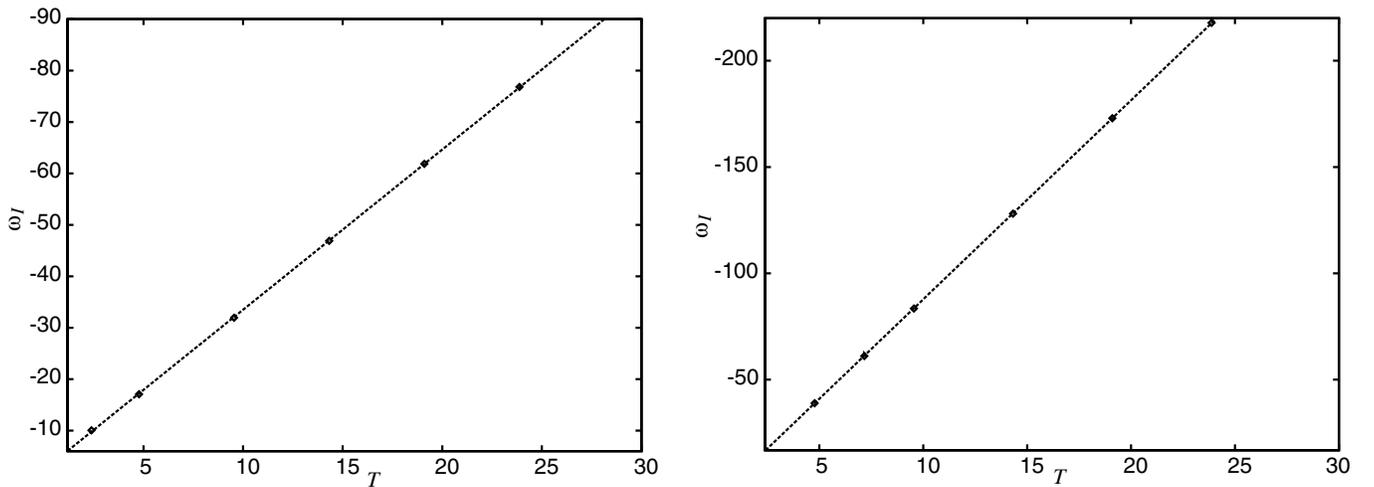

FIG. 2. The imaginary part of the spinor quasinormal mode frequencies for $n = 0, l = 0$ (left) and $n = 1, l = 0$ (right) are shown as functions of the temperature T for some selected black hole sizes. The dots represent some frequencies numerically evaluated. The lines connecting them are linear fits.
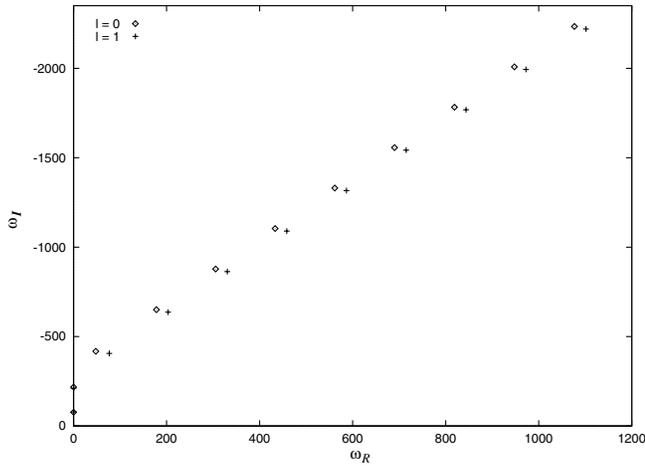
FIG. 3. The frequencies of the first 11 quasinormal modes for the axial component of the Dirac field, are shown for $\alpha^{-1} = 1$, $r_1 = 100$ and the angular mode values $l = 0$ and $l = 1$.
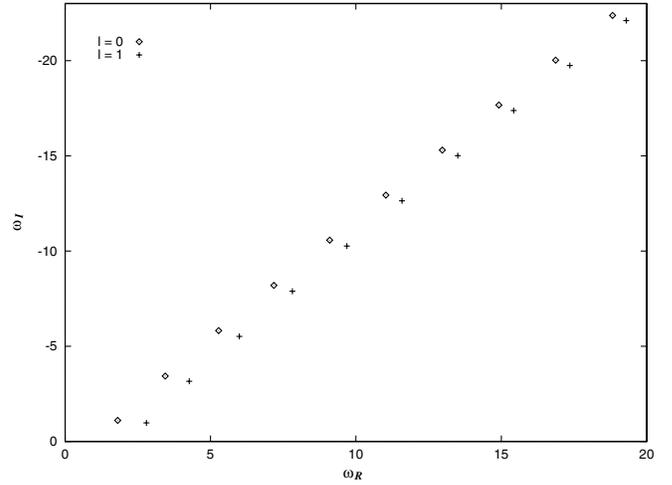

FIG. 4. The frequencies of the first ten quasinormal modes for the axial component of the Dirac field, are shown for $r_1 = \alpha^{-1} = 1.0$, and the angular mode values $l = 0$ and $l = 1$.

higher the number of these first pure damped modes. In Fig. 3, the large black hole frequencies are plotted for $l = 0, 1$.

In Table III, we list the first ten quasinormal mode frequencies corresponding to massless spinor perturbations of intermediate Schwarzschild-AdS black holes ($r_1 \sim \alpha^{-1}$). The values of the frequencies are shown for $\alpha^{-1} = 1.0$ and $l = 0, 1$. For large values of the overtone number n, the modes become evenly spaced and the spacing, which is independent of l, is given by

$$\frac{(\omega_{n+1} - \omega_n)}{r_1} \sim (1.96 - 2.36i). \qquad (4.5)$$

Once again this is a result that, for the intermediate black hole regime, resembles those obtained in [24] for different

kinds of perturbation fields. In Fig. 4, the intermediate black hole frequencies are plotted for $l = 0, 1$.

In Fig. 5 and 6, we show, for intermediate black holes, the dependence of the real and imaginary part of the fundamental quasinormal mode frequencies on the metric parameters for $l = 0$ and $l = 1$. The parameters κ and α^{-1} represent, respectively, the black hole surface gravity evaluated at the event horizon and the Anti-de Sitter radius. Both the real and imaginary parts of the frequencies seem to depend linearly on the black hole surface gravity and therefore on the black hole temperature for $\alpha^{-1}\kappa > 1.8$. This is a result that has already been found in [7] for gravitational perturbations of Schwarzschild AdS black holes. The slopes of the straight lines, which are independent of l, are given by

TABLE III. Quasinormal mode frequencies corresponding to $l = 0$ and $l = 1$ massless Dirac perturbations of an intermediate Schwarzschild-AdS black hole ($r_1 = 1.0$). For large values of the overtone number n, the modes become evenly spaced in mode number and the spacing is given by $\frac{(\omega_{n+1}-\omega_n)}{r_1} \sim (1.96 - 2.36i)$.

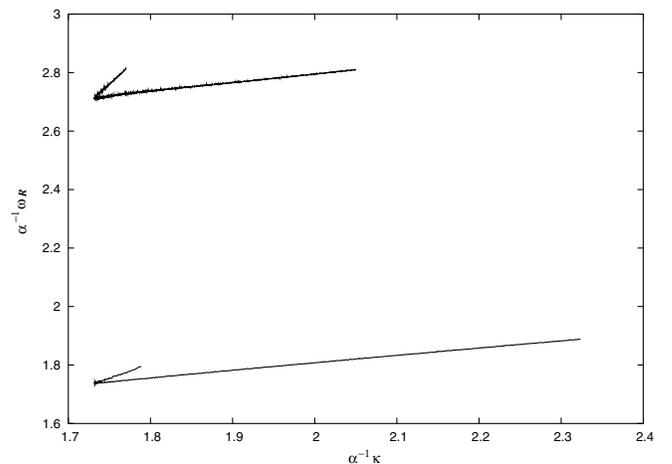| Overtone Number	$l = 0$		$l = 1$	
n	ω_R	ω_I	ω_R	ω_I
0	1.80808	−1.10565	2.7956	− 0.9744
1	3.44229	−3.43805	4.26976	− 3.1623
2	5.28094	−5.82213	5.99062	−5.51618
3	7.17816	− 8.119914	7.81556	−7.89152
4	9.09828	−10.5728	9.68897	−10.2668
5	11.0301	−12.9413	11.5837	−12.6412
6	12.9712	−15.3067	13.5014	−15.0117
7	14.9172	−17.6699	15.4250	−17.3815
8	16.8671	−20.0254	17.3552	−19.7468
9	18.8253	−22.3793	19.2938	−22.1086

FIG. 5. The dependence of the real part of the fundamental quasinormal mode frequencies on the metric parameters for $l = 0$ (bottom) and $l = 1$ (top), is shown for Dirichlet axial boundary conditions on the spinor field.
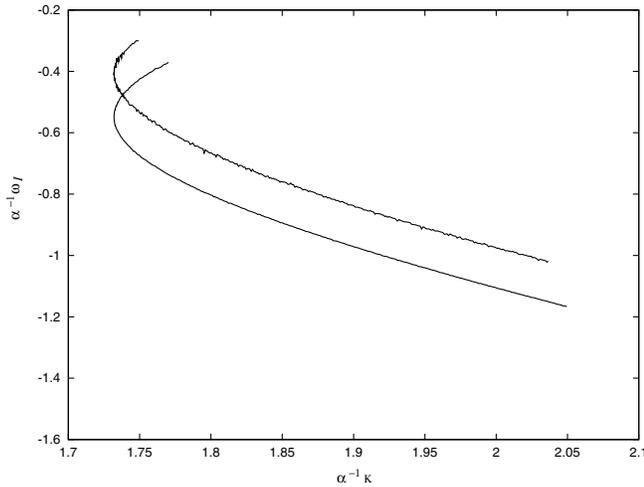
FIG. 6. The dependence of the imaginary part of the fundamental quasinormal mode frequencies on the metric parameters for $l = 0$ (bottom) and $l = 1$ (top), is shown for Dirichlet axial boundary conditions on the spinor field.

$$\omega_R = 0.25\kappa \qquad (4.6)$$

for the plots in Fig. 5 and

$$\omega_I = -1.29\kappa \qquad (4.7)$$

for the plots in Fig. 6.

For small black holes $(r_1 \ll \alpha^{-1})$, it is very difficult to evaluate the corresponding quasinormal frequencies, or to go high in mode number. The error associated in estimating the frequencies in this regime is too high, and we cannot be completely sure of the results. In the case of other perturbation fields [5,6,24], it was found that small black holes have quasinormal frequencies that are very close to the pure AdS values. In the case of the Dirac field considered in this paper, after setting $\alpha^{-1} = 1$, we have been able to evaluate the fundamental frequency, at most, down to the value of $r_1 = 0.3$ (see Table I). Further investigations and more powerful numerical tools are needed to outline the behavior of the spin-1/2 frequencies in the limit of $r_1 \rightarrow 0$.

V. CONCLUSION

In this paper we have investigated the quasinormal mode frequencies of a spinor field interacting with a Schwarzschild black hole in four dimensional Anti-de Sitter space-time. After solving the related axial perturbative equation we have imposed on this solution Dirichlet boundary conditions and evaluated the corresponding quasinormal frequencies. This choice of boundary conditions is physically justified in the contest of the AdS/CFT correspondence, in which it is suggested to exploit these frequencies in the evaluation of poles of correlation functions associated to the conformal field theory on the boundary.

For large black holes, we have numerically confirmed that the imaginary part of the frequency scales with the temperature. We have also shown that both the real and imaginary components of the frequencies are evenly spaced in mode number. The spacing between consecutive modes, which is independent of the angular quantum number l, behaves as in the case of scalar, electromagnetic and gravitational perturbations. The quasinormal frequencies have a number of first overtones with pure imaginary parts.

For intermediate black holes, we have found that both the real and imaginary part of the frequency scale linearly with the surface gravity. The modes are evenly spaced and the spacing, which is independent of the angular quantum number l, resembles the one related to other kinds of perturbations.

Our purpose is to extend this project imposing different boundary conditions on the axial or the polar Dirac equations. We could be interested, for instance, in calculating the correlation functions and associated poles of a quantity related to the axial part of the spinor field. That would suggest we set the polar component of the spinor field perturbation to vanish on the boundary and consequently we could solve either the odd parity differential equation with Dirichlet boundary conditions or the even parity equation with mixed boundary conditions due to the transformation theory between polar and axial functions.

[1] S. Chandrasekhar, *The Mathematical Theory of Black Holes* (Claredon, Oxford, 1983).
[2] H. P. Nollert, Classical Quantum Gravity **16**, 159 (1999).
[3] K. Kokkotas and B. Schmidt, Living Rev. Relativity **2**, 2 (1999).
[4] J. Chan and R. Mann, Phys. Rev. D **55**, 7546 (1997).
[5] G. T. Horowitz and V. Hubeny, Phys. Rev. D **62**, 024027 (2000).
[6] V. Cardoso and J. P. S. Lemos, Phys. Rev. D **64**, 084017 (2001).

[7] I. G. Moss and J. P. Norman, Classical Quantum Gravity **19**, 2323 (2002).

[8] J. Maldacena, Adv. Theor. Math. Phys. **2**, 231 (1998).

[9] U. H. Danielsson, E. Keski-Vakkuri, and M. Kruczeski, Nucl. Phys. B **563**, 279 (1999).

[10] S. Kalyana Rama and B. Sathiapalan, Mod. Phys. Lett. A **14**, 2635 (1999).

[11] D. Birmingham, I. Sachs, and S. N. Solodukhin, Phys. Rev. Lett. **88**, 151301 (2002).

[12] D. T. Son and A. O. Starinets, J. High Energy Phys. 09 (2002) 042.

[13] E. Berti and K. D. Kokkotas, Phys. Rev. D **67**, 064020 (2003).

[14] F. Finster, J. Smoller, and S. T. Yau, Phys. Rev. D **59**, 104020 (1999).

[15] F. Finster, J. Smoller, and S. T. Yau, Phys. Lett. A **259**, 431 (1999).

[16] F. Finster, J. Smoller, and S. T. Yau, J. Math. Phys. (N.Y.) **41**, 2173 (2000).

[17] F. Finster, J. Smoller, and S. T. Yau, Commun. Pure Appl. Math. **53**, 902 (2000).

[18] F. Finster, J. Smoller, and S. T. Yau, Commun. Math. Phys. **205**, 249 (1999).

[19] H. T. Cho, Phys. Rev. D **68**, 024003 (2003).

[20] Jiliang Jing, Phys. Rev. D **69** 084009 (2004).

[21] D. R. Brill and J. A. Wheeler, Rev. Mod. Phys. **29**, 465 (1957).

[22] A. Anderson and R. H. Price, Phys. Rev. D **43**, 3147 (1991).

[23] F. Cooper, A. Khare, and U. Sukhatme, Phys. Rep. **251**, 267 (1995).

[24] V. Cardoso, R. Konoplya and J. P. S. Lemos, Phys. Rev. D **68**, 044024 (2003).